PAPER

Loss Reduction of LLC Converter Using Bridge-Capacitor

Toshiyuki WATANABE[†a)], *Nonmember and* **Fujio KUROKAWA**[††], *Fellow*

SUMMARY Current resonance type of LLC converter is widely used owing to their low switching losses; however, the problem is that they have a large transformer loss. We examine the reduction of AC resistance of the transformer winding and high coupling between the primary and secondary windings of the transformer, as a method for reducing the copper loss. In this case, it is necessary to consider the effects of the increase in stray capacitance between the primary and secondary windings of the transformer. This paper describes the influence of the loss due to the capacitance generated between the transformer windings when a noise filter is connected to the LLC converter. Furthermore, we propose a new method for reducing loss by connecting a bridge-capacitor between the primary and secondary sides of the transformer. The results of the new method are shown, and compared with those of the simulations to demonstrate effectiveness.

key words: *LLC converter, high efficiency, stray capacitance between windings, noise filter, bridge-capacitor*

1. Introduction

In recent years, environmentally-friendly electric vehicles, and IoT (Internet of Things) essential for information society have been promoted. As many switching power supplies are utilized in on-board chargers and power supply units for ICT equipments, their high efficiency, miniaturization, and high power density have become crucial attributes.

To provide these attributes to the switching power supply, a reduction in switching loss is essential. LLC converters are widely used as circuit systems suitable for high efficiency applications [1]–[6]. This is because switching loss can be reduced by soft switching using current resonance [7]–[11].

Although the adoption of soft switching reduces the loss of the switching divice, the application of higher switching frequencies to realize miniaturization and higher power density makes loss reduction of the transformer a big task [12]–[14]. The reduction of copper loss is also essential. In the LLC converter, since the ratio of transformer loss to the entire loss is high in comparison with, for example, a phase shift converter, the reduction of copper loss of the transformer is important to realize higher efficiency [15]. One method for reducing transformer copper loss is to decrease AC resistance at the switching frequency, and the best means is by the use of a planar transformer. The planar transformer can realize an interleaved structure, arranging the primary and secondary windings alternately. The significant reduction of the proximity effect of transformer windings by the interleaved structure can decrease the AC resistance of the LLC transformer. It is recognized that the method for reducing the AC resistance by gain of high coupling of the primary and secondary windings of the transformer, for example by use of a planar transformer, is very effective [16]–[19]. However, the increase in stray capacitance due to the gain of high coupling between the primary and secondary sides of the transformer has an obvious impact [20], [21]. More specifically, harmful effects have been reported due to the increased loss from the generation of circulating currents through this capacitance, and the increased dead time for charging and discharging switch output capacitance to achieve zero voltage switching (ZVS) operation [22], [23].

In addition, there is a problem as losses due to the stray capacitance between the primary and secondary sides of the transformer are generated. Counter-measures for this problem, such as reducing the stray capacitance by inserting a shield layer into the transformer [24]–[26], and reducing the influence of the loss by adjusting the winding layer constitution taking into account the operating voltage between the windings [27]–[30] have been reported. In addition, there are techniques to reduce the common-mode noise using a layered structure that reduces the voltage gradient between the overlapping traces of the transformer, thereby lowering the intrawinding capacitance [31].

Therefore, it is necessary to further understand the influence of the stray capacitance between the transformer windings. When an LLC converter is used in an actual product, a noise filter is conected for EMI (Electro-Magnetic Interference) measures is connected. However, how the stray capacitance between the transformer windings affects this connection is still unclear.

This paper shows that, when an indispensable input/output noise filter is connected to an LLC converter as an EMI measure, a circulating current is generated due to the stray capacitance between the transformer windings and the Y-capacitor of the noise filter, and the loss is generated in the common-mode choke in the noise filter. This circulating current flows through the FG (Frame Ground) and causes electromagnetic interference. Previously, methods for reducing the FG current have been reported for non-isolated converters [32]–[35]; however, it is also necessary to reduce the FG current for the isolated power supplies that use

Manuscript received January 12, 2024.
Manuscript revised May 24, 2024.
Manuscript publicized August 22, 2024.

[†]Shindengen Electric Mfg. Co., Ltd., Asaka-shi, 351-8503 Japan.
[††]Nagasaki Institute of Applied Science, Nagasaki-shi, 851-0121 Japan.
a) E-mail: t_watanabe@shindengen.co.jp

DOI: 10.23919/transcom.2024EBP3012

transformers with large inter-winding capacitance.

In addition, as a method for improving the loss of the common-mode choke due to the stray capacitance between the transformer windings, we propose a new method for connecting a capacitor between the primary and secondary sides of the transformer. This suppresses the circulating current flowing in the noise filter to enable a reduction of the loss. The transformer of the LLC converter used for the on-board charger and the power supply unit for ICT equipment becomes the insulation boundary compliant with safety standards. Since the capacitor across this insulation boundary is defined as a bridge-capacitor [36], this paper also uses the term 'bridge-capacitor'. Although many studies reported on EMI countermeasures utilizing bridge-capacitors [37]–[43], few studies have focused on noise filter loss reduction.

2. Stray Capacitance between Transformer Windings and the Influence of Loss

The circuit diagram of the DC-DC converter section of the power unit for an ICT equipment adopting an LLC converter of the current resonance type is shown in Fig. 1, and the input/output voltage, output power, and operating frequency specifications are shown in Table 1. Figure 2 shows the PWM operating conditions, and Fig. 3 shows the circuit board layout. The output voltage is controlled by adjusting the frequency and the two parallel legs are operated in the same phase.

In the planar transformer used in the LLC converter shown in Fig. 1, the measured values of AC resistance when changing the winding structure of the transformer, as shown in Fig. 4, is as shown in Fig. 6. Figure 5 shows the Physical shape of transformer winding. The measured values of the AC resistance indicate the series resistance of the primary winding with the secondary winding shorted, as measured using an impedance analyzer. The interwinding capacitance of the transformer in Fig. 6 is the capacitance between the shorted primary winding and the shorted secondary winding,

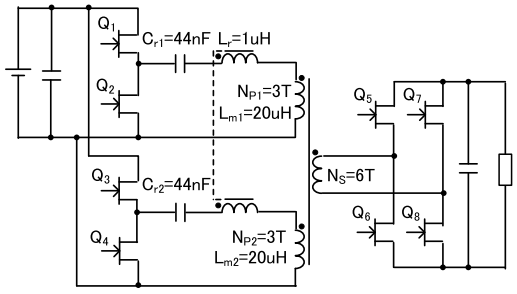

Fig. 1 Basic circuit diagram for LLC converter of current resonance type.

Table 1 LLC converter specification.

Input voltage	Output voltage	Output power	Switching frequency
400 Vdc	383 Vdc	5000 W	600 kHz

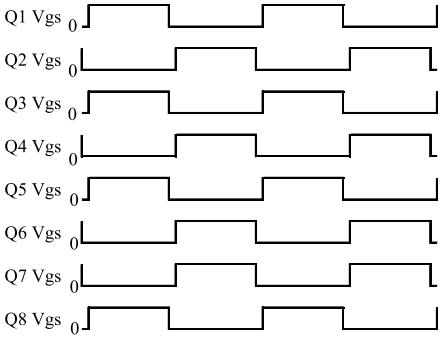

Fig. 2 PWM operating conditions.

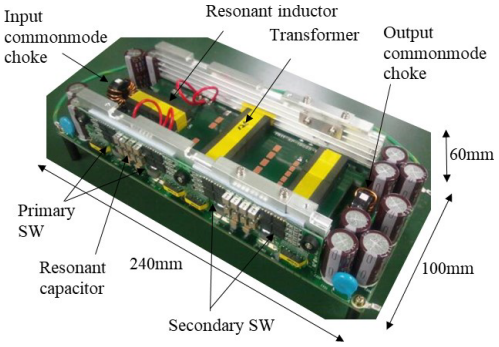

Fig. 3 Circuit board layout of LLC converter.

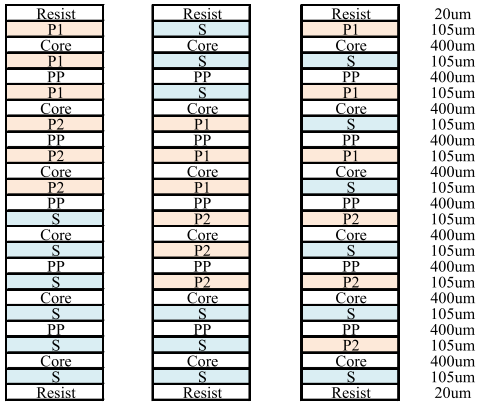

Fig. 4 Winding structure of transformer.

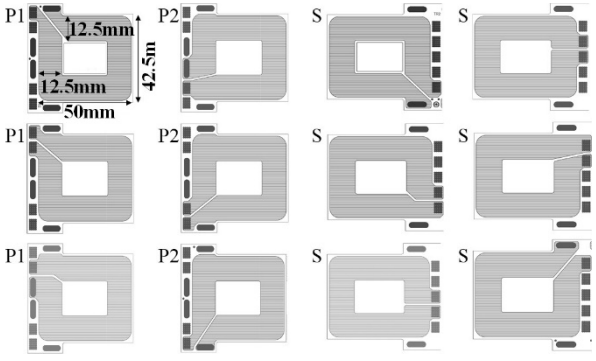

Fig. 5 Physical shape of transformer winding.

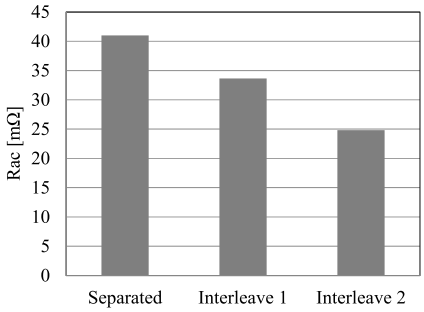

Fig. 6 AC resistance by transformer winding structure (600 kHz).

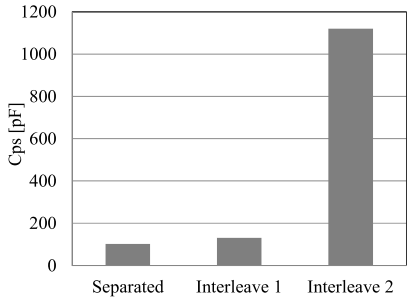

Fig. 7 Capacitance between primary and secondary sides of transformer.

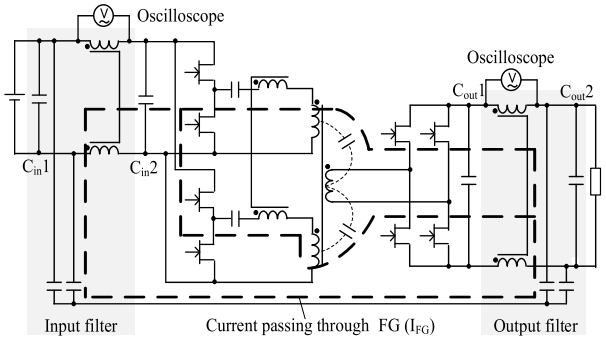

Fig. 8 Circuit diagram including input/output filter.

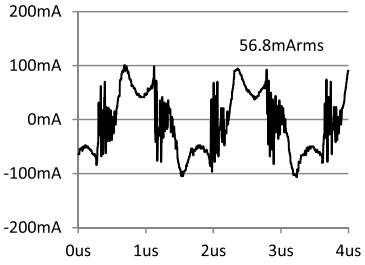

Fig. 9 Waveform of FG passing current (transformer: interleave 2).

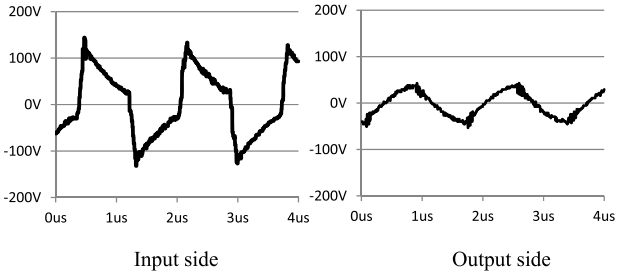

Fig. 10 End-to-end voltage of common-mode choke.

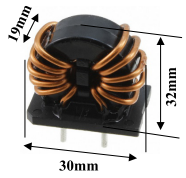

Fig. 11 Physical shape of common-mode choke.

Table 2 Common-mode choke specification.

Number of windings	2
Inductance (common-mode)	74 uH (600kHz)
Inductance (differential mode)	1.3 uH (600kHz)
DC Resistance (each winding)	3.2mΩ
Core material	Nanocrystalline

and is measured using an impedance analyzer. It has been verified that the interleaved structure itself can reduce AC resistance.

The capacitance between the primary and secondary sides of each winding structure of the transformer shown in Fig. 4, is presented in Fig. 7, indicating that the larger the number of interleaves, the larger the capacitance value.

However there has been a concern that the influence of the stray capacitance of the transformer winding generates a circulating current through FG (Frame Ground) and increases the loss of common-mode choke at the input/output filter.

Figure 8 shows the circuit diagram with input/output filtering. While the main purpose of the input filter is to suppress the input feedback noise, the output filter mainly suppresses the noise emitted on the load side; both input and output filters are essential EMI countermeasures.

In such a circuit, when the capacitance between the primary and secondary windings of the transformer increases, a circulating current is generated through the Y-capacitor connected to the FG in the input/output filter, resulting in the loss of the common-mode choke in the filter.

The value of the current flowing in the FG through the Y-capacitor when using the transformer with interleave 2 is shown in Fig. 9.

Figure 10 shows the end-to-end voltage of the common-mode choke of the input/output filter using interleave 2 for the transformer winding structure. The structure of the common-mode choke is shown in Fig. 11, and its specifications are listed in Table 2. It is found that the generation of voltage at both ends of the common-mode choke owing to the common-mode current, results in the iron loss. Subsequently, the temperature rise in the common-mode choke core due to this phenomenon was identified. The end-to-end voltage of the common-mode choke is measured between the terminals of

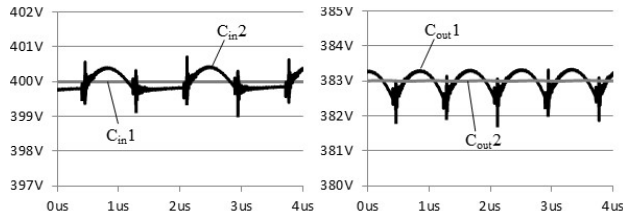

Fig. 12 Capacitor voltage waveforms on both sides of the common-mode choke.

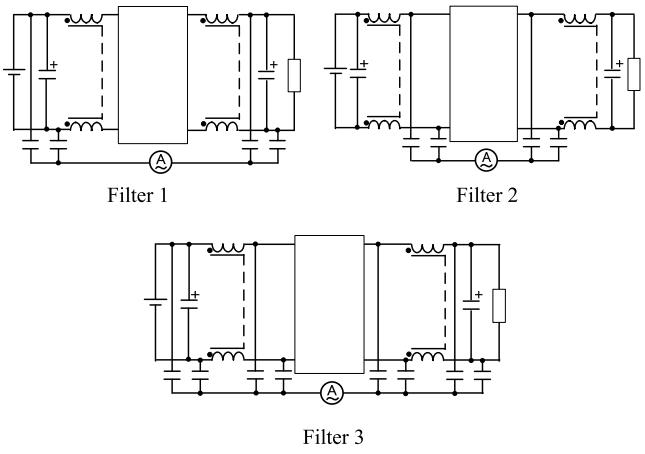

Fig. 13 Connection position of Y-capacitor.

one winding of the common-mode choke using an oscilloscope. Since a differential probe is used, the common-mode choke and oscilloscope are isolated. Figure 12 shows the capacitor voltage waveforms on both sides of the common-mode choke. Since the capacitor voltages on both sides of the common-mode choke are approximately the same, it is believed that the percentage of the differential-mode voltage included in the end-to-end voltage of the common-mode choke shown in Fig. 10 is small.

3. Loss Reduction by Changing the Y-Capacitor Connection Position

As a method for reducing loss in the common-mode choke caused by the circulating current owing to the capacitance between the primary and secondary sides of the transformer, we compared the effects of changing the Y-capacitor connection position, as shown in Fig. 13. The interleave 2 structure with the lowest AC resistance was adopted for the transformer.

Figure 14 shows the measured end-to-end voltage value of the common-mode choke in each filter circuit, and Fig. 15 shows the measured current value flowing in the FG through the Y-capacitor. The capacitance of the Y-capacitor is 4700 pF. Although the change of the connection position in the Y-capacitor is observed to reduce the voltage applied to both ends of the common-mode choke, this method is not suitable for reducing the common-mode choke loss. This is because the circulating current owing to the capacitance between the primary and secondary sides of the transformer increases the current flowing in the FG through the Y-capacitor,

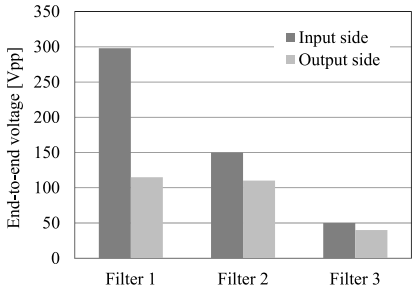

Fig. 14 End-to-end voltage of common-mode choke.

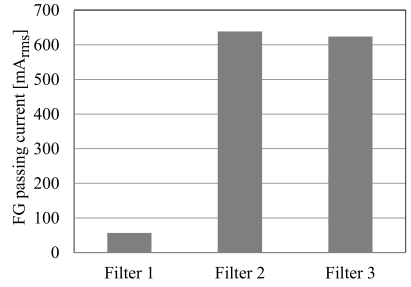

Fig. 15 Y-capacitor connection position and current passing through FG.

which may increase the radiated noise. However, placing a Y-capacitor at a location where the common-mode current passing through the stray capacitance of the transformer bypasses the common-mode choke may reduce the common-mode choke losses.

4. Improvement of Loss by Bridge-Capacitor

By restricting the flow of the circulating current, which is generated from the capacitance between the primary and secondary sides of the transformer, to the common-mode choke and FG, we can suppress the loss of the common-mode choke and the increase in radiated noise. Therefore, we examined the effects of adding a bridge-capacitor between the primary and secondary sides of the transformer.

Because the primary side half-bridge circuit of the basic LLC converter shown in Fig. 1 is a parallel circuit with the same operating current and the voltage at each section, the five candidates are considered for the connection positions of the bridge-capacitor as shown in Fig. 16 (V1–V5, respectively).

Voltage waveforms for V1–V5 in Fig. 16 are shown in Fig. 17, and all waveforms indicate large voltage changes during the switching period. Therefore, there is a concern that the connections of the bridge-capacitor could increase the circulating current.

The addition of a 470 pF capacitor resulted either in a failure of the normal operation of the LLC converter or an increase in input power at no-load. By adding of a capacitor at position V5, a loss reduction effect was obtained. The end-to-end voltage at position V5 presented comparatively smaller fluctuations than that indicated by the voltage waveforms of V1–V4.

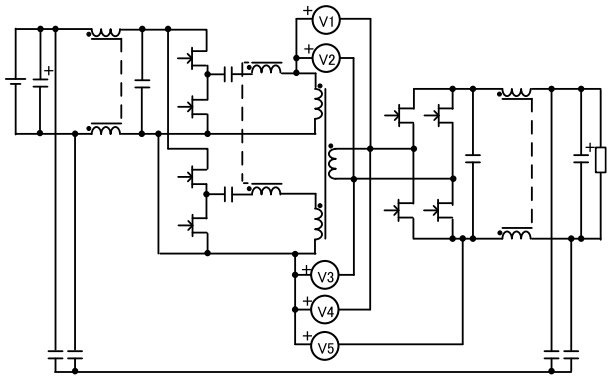

Fig. 16 Connection position of bridge-capacitor.

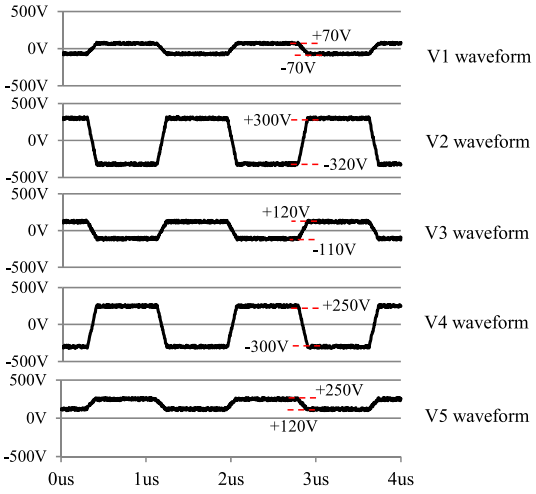

Fig. 17 End-to-end voltage of transformer.

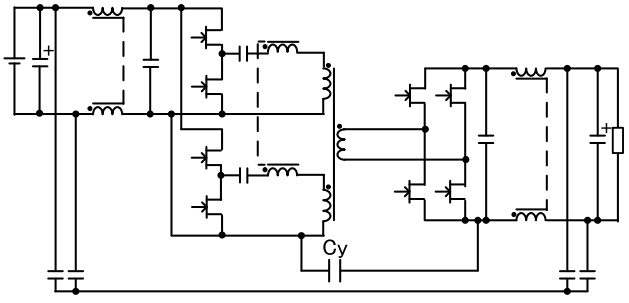

Fig. 18 Proposed connection position for bridge-capacitor Cy.

From the above results, we connected the bridge-capacitor to the position shown by Cy in Fig. 18 (V5 position in Table 3). In on-board chargers and power supply units for ICT equipments, galvanic isolation (double insulation) is required between the primary and secondary circuits of the transformer for safety, the bridge-capacitor must be realized with two capacitors in series. Figure 19 shows the input power at no-load (≈ loss), effective value of the current flowing in the capacitor and effective value of the current passing through FG when changing the capacitance of bridge-capacitor Cy. We verified a reduction in loss of 3.4 W

Table 3 Bridge-capacitor position and loss reduction.

Addition position of bridge capacitor (470 pF)	Input power at non-load	Presence of abnormal operation
None	70.4 W	None
V1	—	No normal operation
V2	—	No normal operation
V3	73.5 W	None
V4	—	No normal operation
V5	69.2 W	None

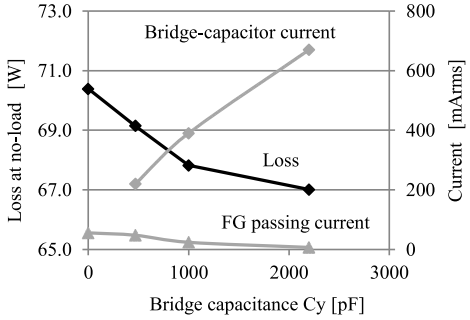

Fig. 19 No-load loss due to capacitance of bridge-capacitor, bridge-capacitor current and FG passing current (measured).

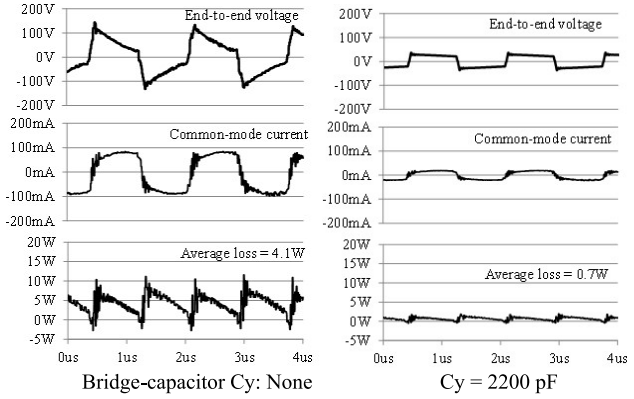

Fig. 20 End-to-end voltage, common-mode current and loss waveforms of input side common-mode choke.

(approx. 4.8% of total loss) with the addition of a 2200 pF capacitor compared to the case of no connected capacitor at all. Although the current flowing in the bridge-capacitor increases in proportion to the capacitance value, increasing the bridge-capacitor capacity reduces the current flowing in the FG through the Y-capacitor. Thus, the influence of radiation noise is thought to be lower.

Figure 20 and Fig. 21 shows the voltage, current, loss waveforms and core temperature of the input side common-mode choke without bridge-capacitor and with a 2200 pF capacitor, respectively. The addition of the bridge-capacitor was found to reduce the loss, and a fall in temperature of the common-mode choke was also identified. The core temperature of the common-mode choke at a 3.5 kW load is considerably lower than before the addition of the bridge-capacitor, indicating that the common-mode choke core temperature rise is caused by the common-mode current and, not the

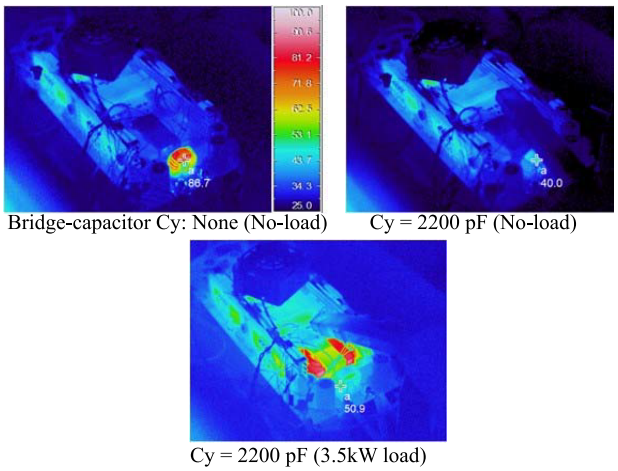

Fig. 21 Core temperature of input side common-mode choke.

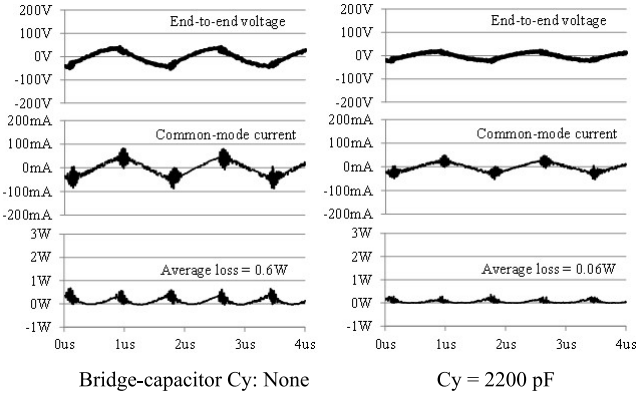

Fig. 22 End-to-end voltage, common-mode current and loss waveforms of output side common-mode choke

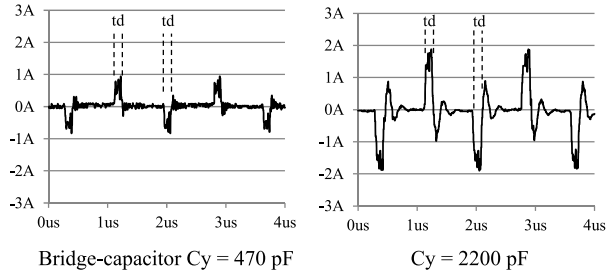

Fig. 23 Current waveforms of bridge-capacitor (measured value).

differential-mode current.

Figure 22 shows the voltage, current, and loss waveforms of the output side common-mode choke without bridge-capacitor, and with the addition of a 2200 pF capacitor. On the output side, the common-mode current is low even in the absence of a bridge-capacitor, and the loss is small. It is necessary to further investigate the reason for the different in common-mode current waveform and that of the input side; for example, whether the common-mode current flows in the control circuit.

Figure 23 shows the current waveforms with a bridge-

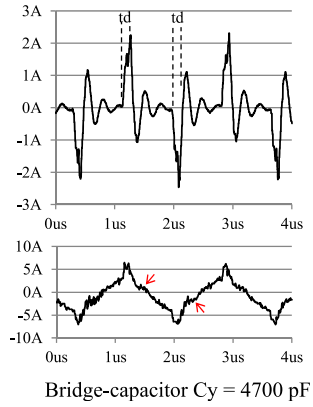

Fig. 24 Current waveforms of bridge-capacitor and primary winding of transformer (measured value).

capacitor of 470 pF and 2200 pF. The current in the bridge-capacitor flows during the dead time (td) when the voltage waveform, (as shown in Fig. 17), changes. When the added capacitance is increased, the resonance of the current continues even beyond the dead time. Figure 24 shows the current waveforms of the bridge-capacitor and the primary winding of the transformer, with a 4700 pF bridge-capacitor.

The increase in the bridge-capacitor up to this value was confirmed to cause the superposition of the current flowing in the bridge-capacitor on the current resonance waveform (section with an arrow). Because this results in the generation of conduction loss in the semiconductor switch, resonance circuit elements, etc., the value of the capacitance that can be added is limited, and optimization is required for loss reduction.

5. Verification by Simulation

Verification of reproducibility by simulation was performed using the circuit shown in Fig. 25. The simulation is performed under the assumption that the experiment and simulation circuits are equivalent because the two legs of primary circuit have the same component ratings and are operated with a same phase. However, additional analysis is required for the influence of small phase errors in the two legs of the primary circuit. LTspice was used as the simulator. Figure 26 shows the transformer electromagnetic field simulation model for extracting the SPICE model. The physical dimensions of the electromagnetic field simulation model are as shown in Fig. 4 and Fig. 5. The transformer circuit simulation model (SPICE netlist) is converted from S-parameters analyzed using the electromagnetic field simulator Ansys HFSS. However, since no common-mode current flows between the primary and secondary windings, the capacitance measured by the forward-winding method [27] is added to the simulation circuit shown in Fig. 25. In order to extract a circuit simulation model in which common-mode current flows between the primary and secondary windings of a transformer, it is necessary to review the analysis method of S-parameter characteristics in electromagnetic field sim-

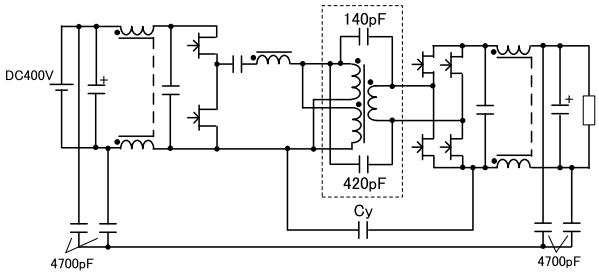

Fig. 25 Simulation circuit.

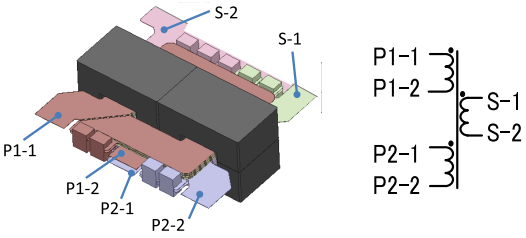

Fig. 26 Transformer electromagnetic field simulation model for extracting SPICE model.

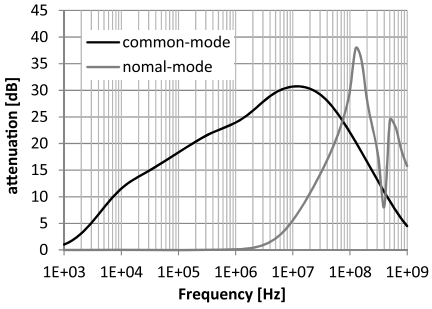

Fig. 27 Attenuation characteristics of common-mode choke model.

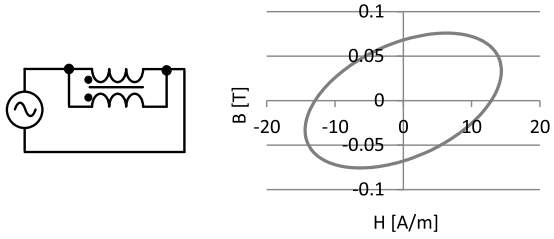

Fig. 28 B-H curve of the common-mode choke simulation model.

ulators. Figure 27 shows the attenuation characteristics (common-mode and normal-mode) of the common-mode choke model used for the filter. The common-mode choke simulation models are provided by the manufacturer. The B-H curve when a 600 kHz, 100 Vpp sine wave is applied to a simulation model of a common-mode choke is shown in the Fig. 28, since the common-mode choke core has hysteresis characteristics, iron loss occurs.

Figure 29 shows the simulated waveforms of the end-to-end voltage of the common-mode choke with different bridge-capacitor values. The addition of the bridge-capacitor

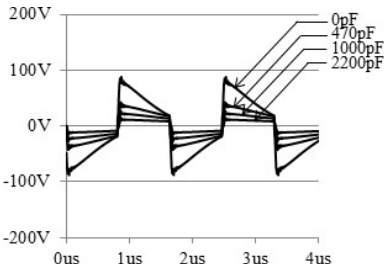

Fig. 29 End-to-end voltage of common-mode choke (Input side).

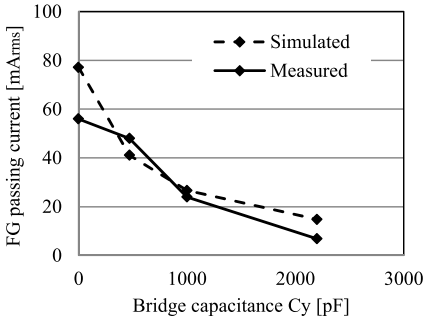

Fig. 30 Capacitance of bridge-capacitor and FG current.

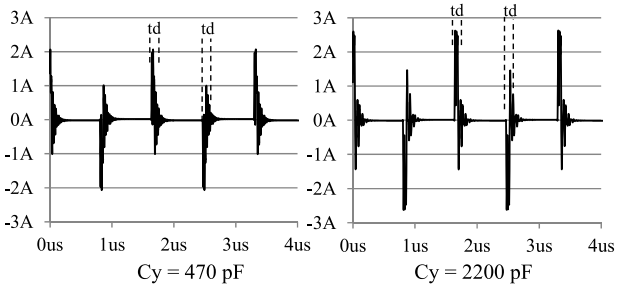

Fig. 31 Current waveform of bridge-capacitor (Simulated value).

suppresses the voltage applied to the common-mode choke. This pattern corresponds to that of the measured waveform shown Fig. 20.

Figure 30 shows the relationship between the bridge-capacitor value and the measured and simulated values of the current passing through the FG. As the addition of the bridge-capacitor suppress the current passing through the FG, the current passing through the input/output filter is also suppressed, thereby reducing in the common-mode choke loss.

Figure 31 shows the simulated waveforms of the bridge-capacitor current with bridge-capacitor values of 470 pF and 2200 pF. Although waveforms with a pattern close to the measured values shown in Fig. 23 were obtained, continuous resonance is observed in the measured waveform of Fig. 23. This is assumed to be due to the difference in the parasitic inductance in the path of the current flow in the bridge-capacitor in the actual circuit and the simulation.

Figure 32 shows the measured and simulated values of the bridge-capacitor current. The tendency of an increase of

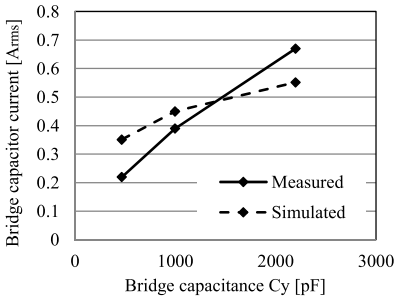

Fig. 32 Current of bridge-capacitor.

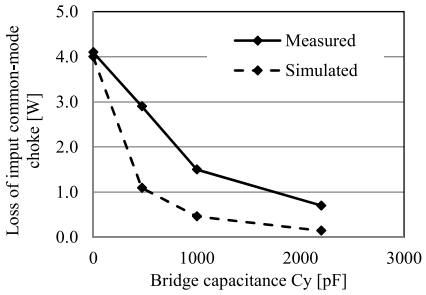

Fig. 33 Capacitance of bridge-capacitor and loss of input common-mode choke.

the current flowing through the bridge-capacitor as the value of the bridge-capacitor increase is consistent with the trend of the measured values. It is believed that the large value measured in the case of high capacitance was caused by the influence of continuous resonance seen in the measured waveform.

Figure 33 shows the relationship between the additional capacitance of the bridge-capacitor and the loss of the common-mode choke. The loss of the common-mode choke was obtained by time integration of the end-to-end voltage of the common-mode choke and the common-mode current.

The loss is reduced because an increase in the value of the bridge-capacitor suppresses the current passing through the FG and decreases the end-to-end voltage of the common-mode choke.

6. Evaluation of the Influence of Noise

Figure 34 shows the simulated circuit of the input feedback noise. We inserted an equivalent circuit of LISN (Line Impedance Stabilization Network) into the input section to perform an FFT of the detected noise voltage. Figure 35 shows the noise reduction effect by the addition of the bridge-capacitor with respect to the 600 kHz fundamental wave component of the switching frequency. A suppression effect of approximately 14 dBuV is obtained when the bridge-capacitor has a value of 2200 pF. Figure 36 shows the frequency characteristics of input feedback noise when a 2200 pF Y-capacitor is connected. By connecting a Y-capacitor, the effect of suppressing high-order harmonic noise of 600 kHz can be obtained.

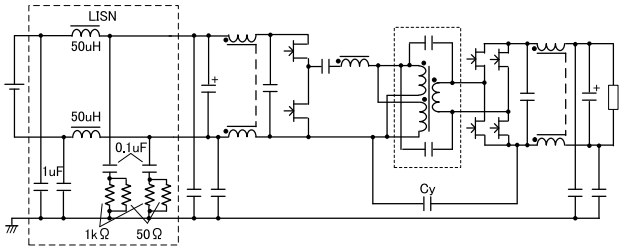

Fig. 34 Input feedback noise simulation circuit.

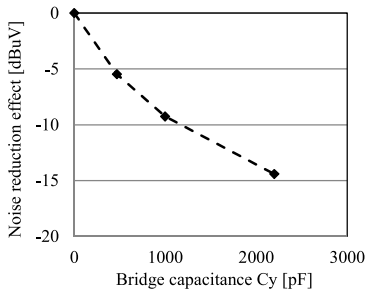

Fig. 35 Effect of noise reduction by addition of bridge-capacitor (at 600 kHz in simulation).

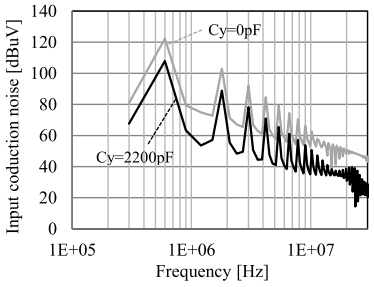

Fig. 36 Frequency characteristics of input conducted noise (Simulated value).

From this result, we successfully verified that the suppression of the current flowing in the FG through the Y-capacitor caused by the addition of a bridge-capacitor also suppresses the emitted noise.

7. Conclusion

In LLC converters, using a transformer with high coupling between the primary and secondary windings and a low AC resistance to reduce the copper loss of the transformer is essential to achieve higher efficiency, smaller size, and higher power density. However, in an LLC converter connected with an input-output noise filter for EMI countermeasures, we pointed out that the following problems arise when using a transformer having high coupling and a high stray capacitance between the primary and secondary sides. We also showed methods to overcome them:

(1) It is shown that a circulating current is generated through the stray capacitance between the transformer windings and the Y-capacitor of the input/output filter, and the

effect that increases the loss of the common-mode choke of the filter was found.

(2) A new method was observed for reducing the loss of the common-mode choke by adding a bridge-capacitor between the primary and secondary sides of the transformer and its reproducibility was verified via simulation.

(3) Adding an optimum value for the bridge-capacitor in the LLC converter connected with an input-output noise filter enabled the reduction of the loss at no-load by approximately 4.8%.

(4) Simulation verification of input feedback noise confirmed that the addition of the bridge-capacitor enabled a reduction of the input feedback noise.

References

[1] O.R. Schmidt and E. Myhre, "380 Vdc/48 Vdc/ 3 kw dc/dc converter with 98.2% efficiency," Proc. IEEE INTELEC, pp.130–135, Oct. 2015.
[2] Y. Jeong, G.W. Moon, and J.K. Kim, "Analysis on half-bridge LLC resonant converter by using variable inductance for high efficiency and power density server power supply," Proc. IEEE APEC, pp.170–177, March 2017.
[3] M. Joung, H. Kim, and J. Baek, "Dynamic analysis and optimal design of high efficiency full bridge LLC resonant converter for server power system," Proc. IEEE APEC, pp.1292–1297, March 2012.
[4] H. Haga and F. Kurokawa, "Dynamic analysis of the three-level LLC resonant converter for a rectifier in HVDC distribution system," Proc. IEEE INTELEC, pp.1–6, Oct. 2015.
[5] Z.J. Su and Y.S. Lai, "On-line DC-link voltage control of LLC resonant converter for server power applications," Proc. IEEE ECCE, pp.5422–5428, Sept. 2014.
[6] Q. Huang, Q. Ma, A.Q. Huang, and M.D. Rooij, "400 V-to-48 V GaN modular LLC resonant converter with planar transformers," Proc. IEEE ECCE, pp.2029–2135, Oct. 2021.
[7] B.C. Hyeon, J.T. Kim, and B.H. Cho, "A half bridge LC resonant converter with reduced current ripple of the output capacitor," Proc. IEEE INTELEC, pp.1–5, Oct. 2009.
[8] K.H. Liu and F.C. Lee, "Zero voltage switching technique in dc-dc converters," IEEE Trans. Power Electron., vol.5, no.3, pp.293–304, July 1990.
[9] K. Liu, R. Oruganti, and F.C. Lee, "Resonant switches, topologies and characteristics," IEEE PESC Record, pp.106–116, June 1985.
[10] B. Yang, F.C. Lee, A.J. Zhang, and G. Huang, "LLC resonant converter for front end DC/DC conversion," Proc. IEEE APEC, vol.2, pp.1108–1112, March 2002.
[11] H. Song, D. Xu, and A.J. Zhang, "Re-analysis on ZVS condition for LLC converter," Proc. IEEE APEC, pp.1874–1880, June 2021.
[12] M. Li, Z. Ouyang, M.A.E. Andersen, "High frequency LLC resonant converter with magnetic shunt integrated planar transformer," Proc. IEEE APEC, pp.2678–2685, March 2018.
[13] S. Yang, S. Abe, and M. Shoyama, "Parametric analysis of LLC resonant converter using flat transformer for loss reduction," Proc. IEEE EPEPEMC, pp.T2-204–T2-209, March 2010.
[14] T. Yamamoto, Y. Bu, T. Mizuno, Y. Yamaguchi, and T. Kano, "Loss reduction of transformer for LLC resonant converter using a magnetoplated wire," Proc. IEEE ICEMS, pp.998–1003, Nov. 2016.
[15] T. Watanabe and F. Kurokawa, "Efficiency comparison between phase shift and LLC converters as power supply for information and communication equipments," Proc. IEEE INTELEC, pp.1–5, Oct. 2015.
[16] J. Zhang, W.G. Hurley, and W.H. Wölfle, "Design of the planar transformer in LLC resonant converters for micro-grid applications," Proc. IEEE PEDG, pp.1–7, June 2014.
[17] H. Choi, K.S. Chung, and G. Li, "Analysis on the loss of hybrid transformer winding for multi-output high frequency (300 W) LLC resonance converters," Proc. IEEE INTELEC, pp.1–4, Oct. 2015.
[18] J. Zhang, W.G. Hurley, W.H. Wolfle, and M.C. Duffy, "Optimized design of LLC resonant converters incorporating planar magnetics," Proc. IEEE APEC, pp.1683–1688, March 2013.
[19] K. Yoshikawa and T. Oshikata, "Planar transformer design of LLC DC-DC converters with electromagnetics simulation," Proc. IEEE ICDCM, May 2019.
[20] R. Prieto, J.A. Cobos, O. Garcia, P. Alou, and J. Uceda, "Taking into account all the parasitic effects in the design of magnetic components," Proc. IEEE APEC, vol.1, pp.400–406, Feb. 1998.
[21] N. Wang, X. Yang, M. Tian, H. Jia, G. Xu, and Z. Li, "An optimal design method considering transformer parasitic capacitance of LLC resonant converters," Proc. IEEE IPEC, pp.998–1003, May 2018.
[22] W. Zhang, Y. Long, Y. Cui, F. Wang, L.M. Tolbert, B.J. Blalock, S. Henning, J. Moses, and R. Dean, "Impact of planar transformer winding capacitance on Si-based and GaN-based LLC resonant converter," Proc. IEEE APEC, pp.1668–1674, May 2013.
[23] N. Wang, H. Jia, M. Tian, Z. Li, G. Xu, and X. Yang, "Impact of transformer stray capacitance on the conduction loss in a GaN-based LLC resonant converter," Proc. IEEE ECCE, pp.1334–1338, June 2017.
[24] Y. Yang, D. Huang, F. Lee, and Q. Li, "Analysis and reduction of common mode EMI noise for resonant converters" Proc. IEEE Applied Power Electronics Conference and Exposition (APEC), pp.566–571, March 2014.
[25] J. Zhang, Y. Wang, and H. Chen, "Design of transformer shielding foil structure for minimizing common-mode noise in LLC resonant converters," Proc. IEEE International Power Electronics and Application Symposium, Nov. 2021.
[26] X. Yu and S. Lin, "EMI characteristic analysis of plane transformer based on LLC circuit," Proc. IEEE International Power Electronics and Application Symposium, Nov. 2021.
[27] T. Watanabe, T. Oshikata, K. Nishijima, and F. Kurokawa, "A new approach of improvement of dissipation caused by capacitance between primary and secondary windings of LLC transformer," Proc. IEEE ICRERA, pp.484–488, Nov. 2015.
[28] M.A. Saket, M. Ordonez, M. Craciun, and C. Botting, "Common-mode noise elimination in planar transformers for LLC resonant converters," Proc. IEEE ECCE, pp.6607–6612, Sept. 2018.
[29] S. Ann, W. Son, J.H. Lee, J. Byun, and B.K. Lee, "Design of a SiC-based LLC resonant converter for on-board chargers considering parasitic capacitance of planar transformer," Proc. IEEE ICEMS, pp.315–319, Nov. 2020.
[30] Y. Cao, P. Ren, X. Huang, Y. Chen, and W. Chen, "Common-mode noise mitigation method for planar transformer based on FB LLC converter," Proc. IEEE APEMC, pp.702–705, Sept. 2022.
[31] M.A. Saket, N. Shafiei, and M. Ordonez, "LLC converters with planar transformers: Issues and mitigation," IEEE Trans. Power Electron., vol.32, no.6, pp.4524–4542, June 2017.
[32] D. Barater, G. Buticchi, A.S. Crinto, G. Franceschini, and E. Lorenzani, "A new proposal for ground leakage current reduction in transformerless grid-connected converters for photovoltaic plants," Proc. Annual conference of IEEE Industrial Electronics, pp.4531–4536, Nov. 2009.
[33] G. Buticchi, G. Franceschini, E. Lorenzani, D. Barater, and A. Fratta, "A novel compensation strategy of actual commutations for ground leakage current reduction in PV transformerless converters," Proc. Annual conference of IEEE Industrial Electronics Society, pp.140–147, March 2010.
[34] Ó. López, F.D. Freijedo, A.G. Yepes, P. Fernandez-Comesana, J.

Malvar, R. Teodorescu, and J. Doval-Gandoy, "Eliminating ground current in a transformerless photovoltaic application," IEEE Trans. Energy Convers., vol.25, no.1, pp.4524–4542, June 2017.

[35] M.H. Hedayati and V. John, "Ground leakage current reduction in single-phase grid-connected power converter," Proc. Intl Aegean Conference on Electrical Machines & Power Electronics (ACEMP), Intl Conference on Optimization of Electrical & Electronic Equipment (OPTIM) & Intl Symposium on Advanced Electromechanical Motion Systems (ELECTROMOTION), pp.107–112, Sept. 2015.

[36] Underwriters Laboratories Inc. (UL), UL Standard for Safety for Information Technology Equipment - Safety - Part 1: General Requirements, UL 60950-1, 2nd ed., Underwriters Laboratories (UL), p.48, 2014.

[37] J.-H. Choi, M. Madafshar, and K. Parmenter, "Designing common-mode (CM) EMI noise cancellation without Y-capacitor," Proc. IEEE Applied Power Electronics Conference and Exposition (APEC), pp.936–940, March 2007.

[38] X. Pingfan, Q. Dongyuan, and Z. Bo, "Conducted EMI suppression method based on obstructing grounding loops," Proc. International Power Electronics and Motion Control Conference (IPEMC), pp.2669–2672, May 2009.

[39] A. Majid, J. Saleem, F. Alam, and K. Bertilsson, "Analysis of radiated EMI for power converters switching in MHz frequency range," Proc. IEEE International Symposium on Diagnostics for Electric Machines, Power Electronics and Drives (SDEMPED), pp.428–432, Aug. 2013.

[40] Y. Bai, W. Chen, R. He, D. Zhang, and X. Yang, "EMI noise cancelation by optimizing transformer design without need for the traditional Y-capacitor," Proc. IEEE Applied Power Electronics Conference and Exposition (APEC), pp.766–771, March 2016.

[41] R.B. Elliott, "Effective, small, and inexpensive common-mode EMI reduction using inverse secondary current cancellation," Proc. IEEE International Symposium on Electromagnetic Compatibility (EMC), pp.542–546, July 2016.

[42] G. Lan, S. Zhang, and X. Wu, "Analysis and reduction of common mode current of the transformer in a full-bridge LLC battery charger," Proc. IEEE Transportation Electrification Conference and Expo, Asia-Pacific (ITEC Asia-Pacific), 5 pages, Aug. 2017.

[43] Y. Bai, X. Yang, D. Zhang, X. Li, W. Chen, and W. Hu, "Conducted EMI mitigation schemes in isolated switching-mode power supply without the need of a Y-capacitor," IEEE Trans. Power Electron., vol.32, no.4, pp.2687–2703, April 2017.

Toshiyuki Watanabe received the B.E. degree in Electrical and electronic engineering from Chiba University, Chiba, Japan, in 1995. He is now with Shindengen Electric Mfg. Co., Ltd. He received the Ph.D. from Nagasaki University, Nagasaki, Japan, in 2020. His current research area is highly efficiency power supplies.

Fujio Kurokawa received a B.S. degree in electronic engineering from the Fukuoka Institute of Technology, Fukuoka, Japan, in 1976, and a Dr. Eng. Degree from Osaka Prefecture University, Sakai, Japan, in 1988. Since 2017, he has been with Nagasaki Institute of Applied Science, and is currently a professor at the Institute for Innovative Science and Technology. His research and teaching interests are in the area of dc-dc converters, ac-dc converters, inverters and their digital control, renewable energy technologies, power electronics technologies in aerospace applications and automobiles, and switching power supplies for lighting systems. Prof. Dr. Kurokawa is a Fellow of IEEE, a Fellow of the Illuminating Engineering Institute of Japan, and a senior member of the Institute of Electrical Engineers of Japan.